PROBABILISTIC ANALYSIS OF CRACKING IN CONCRETE FLOOR SLABS UNDER SEISMIC LOADING AND INTERACTIONS WITH POWER ACTUATED FASTENERS (PAF)

A. Yousef[1], P. Spyridis[2], P. Grzesik[3] & K. Bergmeister[4]

[1] Technical University of Dortmund, Dortmund, Germany, alhussain.yousef@tu-dortmund.de

[2] University of Rostock, Rostock, Germany

[3] Hilti Corporation, Schaan, Liechtenstein

[4] Institute of Structural Engineering (IKI), Vienna, Austria

Abstract: *Power Actuated Fasteners (PAF) are commonly used in construction for non-structural applications like fixing electrical components or installing drywall partitions mounted on either side of concrete floor slabs in seismic and non-seismic regions today. They are known for their efficiency and cost-effective installation process. However, the behavior of PAF under seismic conditions is not fully understood, and there is a lack of seismic qualification criteria for such systems. This paper presents a probabilistic analysis of cracking in concrete slabs assuming seismic design situations and interactions with PAF. For this investigation, a model was programmed to predict the expected crack pattern due to various limit states. The model integrates a large database of standard materials and allows for various geometric and material configurations of the concrete slab, reinforcement steel, and boundary conditions. The calculation of the cracks is based on widely acknowledged equations, in line with Eurocode 2. These are then integrated into stochastic models with randomly generated parameters as input for iterations assuming common concrete floor slab configurations. The assumed boundary conditions under various load conditions, are linked to earthquake situations and they provide insights into the likelihood of an interaction between PAF and cracks in concrete slabs. The investigation was concluded by conducting tests against three specific limit states: diaphragm shear, reinforcing steel, and a selected sample of shear resistance elements, namely shear walls connected to the diaphragm. The results of the investigation revealed a range of crack widths that occurred as a result of applying these limit states, which may be considered for future seismic pre-qualification testing of PAF.*

1. Introduction

Fastening systems offer an efficient means to attach both structural and non-structural elements to steel and concrete substrates. Their behavior and load-bearing capacity can be significantly influenced by cracks in concrete. The development of cracks, particularly in seismic conditions, follows the normative crack model only to an expected extent, introducing a certain level of uncertainty. This uncertainty must be considered when designing a safe and reliable fastening system. A stochastic investigation becomes crucial to examine the anticipated characteristics of all potential cracks and their intersections with fastening systems.

1.1. Overview and paper innovation

The study presented herein, addressed the comparison and analysis of recognized theoretical models for crack width calculation with a focus on earthquake-related design situations for floor slabs and the load-bearing performance of installed PAFs. To do so, a MATLAB-based calculation tool is designed to allow a flexible definition of geometrical and material configurations, boundary conditions or loads on floor slabs, and multiple nail-set sizes and nail group configurations. This tool calculates crack widths and spacings under various geometric and material boundary conditions and it serves to delve deeper into the influence of significant parameters.

The flexural cracks in the slab due to the vertical component of an earthquake can be calculated assuming stresses at the onset of yielding of steel (for typical steel rebars in Europe f_y=500MPa) as a worst-case boundary condition. The yield moment can be calculated due to the geometrical, material inputs, and support conditions of the slab.

The calculation model for cracks due to in-plane shear forces is based on the strut and tie method. In this method, the lateral force acting on the slab can be conveyed to tension and compression trajectories in the plane of the slab. The model allows three slab boundary conditions (simply supported slab, fixed slab, and cantilever). After defining the tensile forces in the slab, the crack widths and spacing can be calculated according to the normative crack model, as e.g. applicable in the European standard EN 1992-1-1, with additional boundary conditions related to seismic loading as per DIN EN 1998-1, where necessary.

For the validation of the developed model, nonlinear finite element analysis (NLFEA) has been employed. NLFEA is a powerful tool for modeling the complex behavior of concrete, including cracking. It is effective in predicting the load-deflection response, determining the location and width of cracks in concrete structures, and enabling realistic representations of concrete element failure based on various constitutive models (smeared and discrete cracking, plasticity, damage mechanics). In the NLFEA software ATENA, utilized in this study, the tensile behavior of concrete is described through smeared cracks, crack band, and fracture energy, while the compressive behavior is captured by a plasticity model with hardening and softening. Cervenka (2013) provides a detailed description of the validated constitutive model implemented in the ATENA software, demonstrating a numerical investigation of crack propagation in a shear wall within the CONCRACK workbench.

For the probabilistic approach, 10,000 positions of nail-sets are randomly generated for each investigated slab configuration. Following this, the distance of each nail to the nearest crack is calculated, leading to the generation of an output database. This database serves as a reference for the evaluation of fixing non-structural components, such as partition walls, in seismic scenarios.

1.2. Concrete cracking during earthquake and its influence on fastenings

Cracks in concrete are a common phenomenon that frequently develops because of stresses that exceed the tensile strength of the concrete. Cracks in concrete can vary from being non-structural and unsightly, to being detrimental to the durability, structural safety and integrity of the building. In addition, the behavior of non-structural elements and their attachments is under scrutiny globally and concrete cracking may lead to adverse effects to nearby fasteners.

The stresses causing cracks in concrete can be imposed by the different kinds of loads to which a structure can be subjected. Under seismic loading, the dynamic mass of the structural elements is activated, and the load actions can be significantly higher than under static conditions. The structural elements are subjected to the horizontal and vertical components of seismic accelerations. A seismic force-resisting system like shear-walls or moment frames in structural buildings usually resist the horizontal component of an earthquake. However, horizontal concrete slabs are also subjected to these horizontal forces, which can lead to in-plane diaphragm shear stresses. An earthquake's vertical components in addition to gravity loads can cause an increased bending moment in reinforced concrete slabs, leading to additional stresses on rebars.

During earthquakes, structures experience displacements that result in deformations of their individual members. These deformations lead to the formation and opening of cracks in the members. When the direction of the displacement of the structure changes, moment reversal will occur in some members, and cracks that had been opened during a previous displacement cycle will be closed.

Many analytical models and investigations for crack widths and spacings were used to establish the calculation tool. The focus was on the normative models since they are already known and applicable. In Marti et al. (1998) the tension cord model was discussed and presented with its application for a unified treatment of cracking, minimum reinforcement, tension stiffening, and deformation capacity of non-prestressed and prestressed concrete members. The article also discusses concrete's in-plane stress problem. The work in Kaufmann, W. (1998) presents a new model for cracked orthogonally reinforced concrete panels subjected to a homogeneous state of in-plane stress. The cracked membrane model combines the basic concepts of the original compression field approaches and the tension chord model. Crack spacings and tensile stresses between the cracks are determined from first principles and the link to limit analysis methods is maintained since equilibrium conditions are expressed in terms of stresses at the cracks rather than average stresses between the cracks as in other approaches.

When it comes to fastenings, the concrete crack widths of reinforced concrete members resisting seismic loads are often not clear and can only be determined to a limited extent with analytical models. Thus, an increasing number of investigations regarding practical crack width calculations and subsequent approaches with simulative and mechanical models were researched and evaluated already in the past, with a focus on beams and columns.

The crack width associated with this behavior during an earthquake significantly influences the behavior of fasteners. Hoehler (2006) investigates the conditions to which fasteners may be subjected during an earthquake so that realistic boundary conditions and maximum crack widths for testing can be established. It is shown that fasteners used to connect structural and non-structural elements to a reinforced concrete structure experience both crack cycling and load cycling at dynamic rates during an earthquake. The work also establishes typical values for crack widths and the number of crack opening and closing cycles during an earthquake. These values can be used in fastener qualification tests based on theoretical considerations and numerical studies. The focus of the dissertation is on beams and columns. It also shows that the largest cracks occur at a high aspect ratio and cracks are smaller at low aspect ratios, as found in slabs. This work also demonstrates that some existing design guidelines have an insufficient margin of safety to avoid brittle fastener failure.

Faraone, G et al. (2019) presents an experimental investigation of the behavior of post-installed anchors during the developing of shear-flexural cracks in a shear wall. The work demonstrates that the coupled shear and flexure behavior dominated the response of the wall specimen. While Hoehler (2006) focuses on beams and columns under flexural loading close to plastic hinges and Faraone, G et al. (2019) on shear walls, the experimental tests in Avellaneda, R et al. (2021) were conducted to examine the distribution and width of the cracks that form as the end bay of the diaphragm is subjected to shear angles that are associated with design earthquake (DE) and maximum considered earthquake (MCE) hazard levels. The cracking behavior of unreinforced and reinforced concrete-filled steel deck diaphragms, as well as a cast-in-place reinforced concrete diaphragm, were presented and discussed.

1.3. Power actuated fasteners (PAFs)

Direct fastening technology is a technique in which specially hardened nails (Figure 1a) or studs are driven into steel, concrete, or masonry by a piston-type tool (Figure 1b), without the need for a pre-drilled hole. Materials that can be fastened to concrete or steel by this method are sheet steel, wood, insulation, and some kinds of plastic parts. Fastener driving power is generated by a powder load (a cartridge containing combustible propellant powder, also known as a “booster” (Figure1c)), combustible gas, or by a battery-driven mechanism. During the driving process, the base material is displaced and not removed. In light-duty steel and concrete applications, power-actuated fasteners (PAF) are commonly used. By using the tool and driving energy, fasteners can be driven directly into concrete without the need for a pilot hole. One of the common uses of the direct fastening is to attach wall partition tracks to concrete floors or walls (Figure 2).

Direct fastening by the use of nail-type Power Actuated Fasteners (PAFs) is an efficient and economical method for attaching non-structural components or elements to steel and concrete. in general, the nature of load bearing of such fasteners is governed by high sensitivity to the impact-type setting and the substrate irregularities close to the surface (e.g. hard aggregates or local material defects), whilst the size of the fastener can lead to a relatively low single-point capacity. Therefore, common statistical evaluation and design safety concepts based on single characteristic resistance values are not applicable in the design. Nonetheless, PAFs allow a very efficient installation technique characterised by speed, ease and versatility for various substrates and fixtures, but also health and safety benefits as the absence of electrical supply at the work area, noise, and vibrations. Moreover, the high variability in the resistance of single PAFs is facilitated by the implementation of multiple fasteners and system redundancy, which allow a safe performance in groups of four or more fasteners also for demanding safety critical applications.

Figure 1. a: magazine loaded nail X-P 27 MX (Hilti), b: Hilti Power-actuated direct fastening tool, c: Hilti powder cartridge for direct fastening.

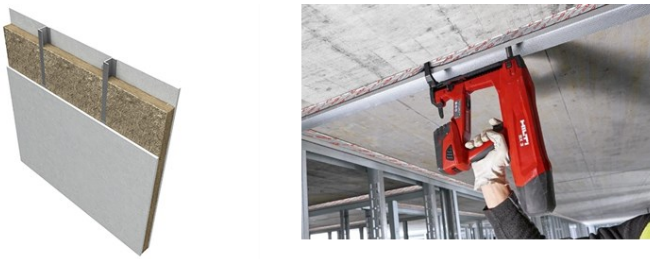

Figure 2. Application of direct fastening in attaching partition wall track to concrete slab.

1.4. Non-structural applications of PAFs and its behaviour under seismic excitation

PAFs are frequently employed in light-duty applications for attaching non-structural components, including partition walls, exterior wall tracks, and suspended ceilings. The focus here is on PAFs application for interior partition walls, given their vulnerability to seismic damage and extensive utilization of PAFs for attaching drywall tracks to concrete.

Building contents and non-structural components play a crucial role in performance-based earthquake engineering. The cost of these items is a major portion of the building's total cost in most buildings. Potential losses to owners will be largely incurred by the non-structural parts of the building after an earthquake Taghavi, S (2003). Particularly interior partition walls are prone to earthquake damage, and they represent a significant investment. Currently, ASCE 7 (2016) commentary suggests that PAF may be prone to pull-out when the concrete slab cracks during seismic excitation, although insufficient data exists to evaluate this behavior under seismic excitation. Furthermore, seismic qualification criteria do not currently exist for such fastening systems, and applying criteria for single-point anchors may not adequately address the behavior and use of such fastening systems Eatherton, M et al. (2006). A detailed investigation to determine crack widths for floor slabs subjected to diaphragm action is not available and therefore required. Besides the experimental tests, the numerical models offer a probabilistic and stochastic evaluation of the crack widths, spacings, positions, and directions and can lead to a better comprehension of the behavior of the fastening systems in the concrete diaphragms under the seismic action.

1.5. Structure of the paper

Since the load-bearing capacity of direct fasteners can also be strongly affected by cracks in the concrete, this paper deals with the stochastic analysis and statistical evaluation of the PAF interaction with a cracked concrete floor slab, particularly in the case of earthquake excitation.

Chapter 2 provides the theoretical foundation, incorporating the strut and tie model (STM) for stress paths in slab planes and the normative crack model from the Euro Code 2, along with assumptions made for this stochastic investigation. Chapter 3 outlines the structure of the MATLAB model, while Chapter 4 conducts a comparative assessment of the MATLAB model results with the non-linear finite element ATENA and laboratory experiments. Chapter 5 presents a parametric and probabilistic evaluation of common concrete slab configurations. Finally, Chapter 6 offers conclusions drawn from the study.

Figure 3 demonstrates the amalgamation of diverse theoretical foundations with a self-developed model for generating nail positions and calculating nail-crack distances. This illustrates the convergence of these elements, contributing to the outcomes of the analysis.

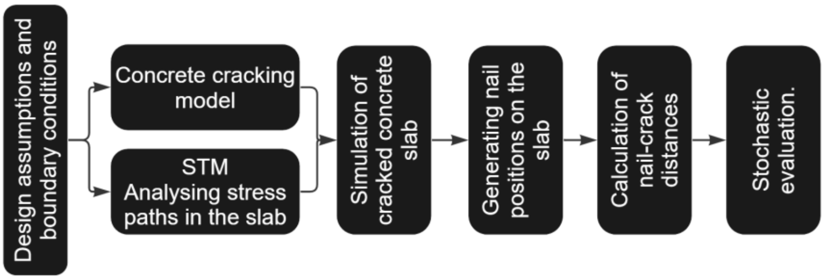

Figure 3. Integration of the theoretical foundations within the model.

2. Theoretical background of the Model

2.1. Strut and tie model

Strut and tie modelling (STM) is a simple method that effectively expresses complex stress patterns as triangulated models. It is based on the fact that concrete and steel convey compression and tension stresses (hence forming fictive struts and ties) respectively. It is usually employed to design non-standard elements or parts of elements of concrete structures such as pile caps, corbels, deep beams (where depth > span/3), beams with holes, connections, etc. where normal beam theory does not necessarily apply, facilitating simple engineering solutions to complex structural problems, while it is acceptable by most current structural design standards. The state-of-the-art of STM and its application to numerical analysis are presented in Fib bulletin (2021). STM is a lower-bound plastic theory which means it is safe providing that, (i) equilibrium is satisfied, (ii) the structure has adequate ductility for the assumed struts and ties to develop, (iii) struts and ties are proportioned to resist their design forces. The design process for strut-and-tie models can be summarised into four main stages:

1. Define and isolate B- (i.e., beam or Bernoulli) and D- regions (disturbed or discontinuity).
2. Develop an STM - a truss system to represent the stress flow through the D-region and calculate the member forces in the truss.
3. Design the members of the STM - dimension and design the truss members to resist design forces.
4. Iterate to optimize the STM as necessary to minimize strain energy.

2.2. DIN EN 1992-1-1 model of cracking in concrete

The crack width calculation model used in Eurocode 2 is mainly based on scientific research results and optimizations by König and Tue (1996). This model, which has been further developed over the years, is currently the state of the art in Europe and it is used to calculate the characteristic (95% fractile at rebar level) crack width. The crack spacing and the strain difference between the mean strain of the reinforcement and the mean strain of the concrete between the cracks are determined in the model based on mechanical semi-empirical equations. The crack width is then obtained by multiplying the strain difference and the crack spacing. The equations are as follows:

Maximum expected crack spacing:

$$s_{r,max} = k_3 \cdot c + k_1 \cdot k_2 \cdot k_4 \cdot \frac{\emptyset}{\rho_{p,eff}} \tag{1}$$

Strain difference:

$$\varepsilon_{sm} - \varepsilon_{cm} = \frac{\sigma_s - k_t \cdot \frac{f_{ct,eff}}{\rho_{p,eff}} \cdot (1 + \alpha_e \cdot \rho_{p,eff})}{E_s} \geq 0,6 \frac{\sigma_s}{E_s} \tag{2}$$

Characteristic crack width:

$$w_k = s_{r,max} \cdot (\varepsilon_{sm} - \varepsilon_{cm}) \tag{3}$$

If the spacing between the steel rebar exceeds the value: $5 \cdot (c + \frac{\emptyset}{2})$ or when there are no rebars in the tensile zone in the concrete, the maximum crack spacing can be calculated as in equation (4):

$$s_{r,max} = 1{,}3(h - x) \tag{4}$$

Equation (5) shows the calculation of the diagonal crack spacing due to a calculated crack spacing in two direction x and z based on the euro code 2:

$$s_{r,max} = \frac{1}{\frac{\cos\theta}{s_{r,max,x}} + \frac{\cos\theta}{s_{r,max,z}}} \tag{5}$$

ere: θ: is the angle between the x- direction and the principal stress; $S_{r,max,x}$, $S_{r,max,z}$: are the maximum crack spacing In both directions x and z; c: concrete cover; $\rho_{p,eff}$: reinforcement ratio; ϕ: rebar diameter; k_1: coefficient for consideration of the composite properties of the reinforcement; k_2: coefficient for consideration of the strain distribution; k_3 & k_4: country specific values; k_t: coefficient dependent on the duration of the load; σ_s: stress in steel; $f_{ct,\,eff}$: effective tensile strength of the concrete; E_s: elasticity modulus of steel; E_{cm}: elasticity modulus of concrete; a_e: the ratio E_s/ E_{cm}; ε_{sm}: the mean strain in the reinforcement under the relevant combination of loads; ε_{cm}: the mean strain in the concrete between cracks. The concrete tensile strength contribution is limited to max. 40 % of the reinforcement stress, there is a load rate-related coefficient, the degree of reinforcement, and the ratio of the modulus of elasticity. Resulting crack widths are to be understood as characteristic values at the level of reinforcement.

2.3. Model assumptions

Due to the equal displacement concept, mentioned in Rodriguez, M et al. (2007) which states that the peak displacement of a long-period structure will be similar when subjected to an earthquake ground motion regardless of whether the system is elastic or inelastic, the concrete in the model is assumed to be super-elastic. The flexural shear cracks due to the in-plane shear force are neglected and only the diagonal cracks are recorded and evaluated.

Level of the calculated cracks

Considering the practical parameters of embedment depths ranging from 17 to 38 mm and concrete covers of 20 to 45 mm (where 20 mm is a common minimum value for dry interior conditions, where PAFs are prevalent), the installed PAF's nail tip is located around the level as the steel rebar in the concrete diaphragms. It is reasonable to approach the crack width at the level of the rebars, as the anchorage of PAFs is primarily located closer to the tip rather than the nail head, where the concrete may be somewhat damaged during installation. The anchorage dominates at the nail tip due to the high temperature during the driving process, which melts the zinc and bonds it to the concrete, as well as clamping and micro keying Hilti (2021).

Assumption for the flexural loads

Since the crack widths are proportional to the strain of tension steel and the crack spacing S_{rmax}, the flexural cracks will be calculated assuming stresses near the rebar yielding in the middle of the slab and with the assumption, that the cracks occur in maximum crack spacing. This conservative assumption is necessary to evaluate the maximum expected cracks in the ultimate state of the slab.

Assumptions of the Shear loads

For the probabilistic analysis, two limit states were investigated concerning the planar shear load: diaphragm shear strength and the yielding of steel rebar due to in-plane shear, respectively. In P. Moehle et al (2010) the predicted shear strength of the diaphragm can be calculated as follows:

$$S_n = \Phi.\ b.d_c\ (2.\lambda.f_c{}'^{0.5} + \rho_t f_y) \tag{9}$$

Where: b: unit width of the diaphragm. d_c: concrete slab thickness. λ: modification factor to reflect the reduced mechanical properties of lightweight concrete relative to normal-weight concrete of the same compressive strength per section =1. f_c ‘: specified concrete compressive strength. ρ_t: ratio of cross-sectional area per unit width of reinforcing steel bars parallel to the direction of diaphragm shear to the unit area of concrete. f_y: specified minimum yield strength of reinforcement. Φ: The appropriate resistance factor in accordance with

=0.75. Based on the findings from a typical floor in it was observed that the elastic diaphragm resistance during the design earthquake exceeds the design demand by a factor of two. Consequently, an investigation into crack widths was conducted at the level where the reinforcement steel in the diaphragm begins to yield due to the in-plane shear force.

3. Model structure

The MATLAB model is composed of various subroutines designed for calculating flexural and shear cracks and conducting probabilistic analyses. Within the "Input" subroutine (Figure 4a), users can input fundamental parameters and boundary conditions for the calculations. This includes specifying the geometric and material properties of the slab's cross-section and rebar, determining the element size, and selecting the safety level for processing the strut and tie model. Once all the necessary data is provided, the calculation of the yielding moment in the center of the slab can proceed (Figure 4b).

In the "Strut and tie model" subroutine (Figure 4c), the applied external force is transformed into compression (struts) and tension (ties) paths. This step is crucial for calculating shear cracks in the model. Essential inputs for this calculation include geometric and material properties, the magnitude and position of externally applied forces, and the slab's boundary conditions. The results of this subroutine yield values and trajectories of the compression and tension forces within the slab's plane.

Once the yield moment and the planar shear forces within the slab have been computed, the model proceeds to calculate shear and flexural cracks. For the diagonal cracks due to shear forces, the diagonal crack spacing can be calculated due to equation (5). Special attention is given to the intersection zone where shear and flexural cracks intersect. This consideration is vital because in this area, the cracks may have greater widths than in sections where only shear or flexural cracks exist (Figure 4d). Following the calculation and generation of cracks on the slab, the position of nails on the slab will be randomly generated to facilitate the probabilistic approach. Nails will be generated in sets, with each set containing five nails. Typically, for the installation of partition walls, three different sizes of nail sets are employed, offering spacing options of 0.2 meters, 0.3 meters, or 0.6 meters between each nail within the set. It's important to note that the size of the nail set can be defined within this subroutine (Figure 4e).

During the probabilistic evaluation phase, various statistical operations are carried out on the dataset. These operations encompass tasks such as identifying the nails within the influence zone of the cracks (45mm from each side of the crack, based on experimental tests conducted at the laboratories of the Technical University of Dortmund) associating the crack width values with the corresponding nails, and representing the data using histograms and plots to facilitate visualization and analysis. Figure 5a illustrates the analysis of stress paths within the planar structure of the slab, while Figure 5b demonstrates the calculation of diagonal cracks in the slab's plan. Following the generation of 10,000 random nail positions on the slab, with a density of 630 nails per square meter (m^2), Figure 5c displays the captured nail positions within the influence zone of the calculated cracks. Nails situated in the white area are outside the influence zone of the cracks and are consequently considered to be in non-cracked concrete.

4. Model verification

To validate the accuracy of the calculation tool used for determining crack widths and spacing, a series of cross-check validations and comparisons were conducted as follows:

4.1. Comparative assessment for the shear cracks with results from Virginia Tech

In Avellaneda, R (2021), a cantilever diaphragm test was conducted on a 4.57 m x 3.65 m reinforced concrete floor diaphragm specimen. Crack widths were measured at four key times during simulated seismic tests. The calculation tool replicated the cantilever, incorporating specimen properties and load conditions. Figure 6 compares test and model results at 2/3 peak shear strength, resembling a design earthquake level, which is often used for non-structural element design. Results demonstrated good agreement between the model and test, including identifying areas with varying crack widths. In the MATLAB model, the maximum crack width is 0.6 mm, the minimum is 0.3 mm, and the typical width is 0.5 mm. In Avellaneda's experimental tests, the maximum crack width reaches 1 mm, the minimum is 0.25 mm, and the typical range is 0.4-0.6 mm. It's noteworthy that the maximum crack widths in the test were observed where the slab connected to supporting beams with welded shear studs, a location typically not the primary site for interior partition wall installations.

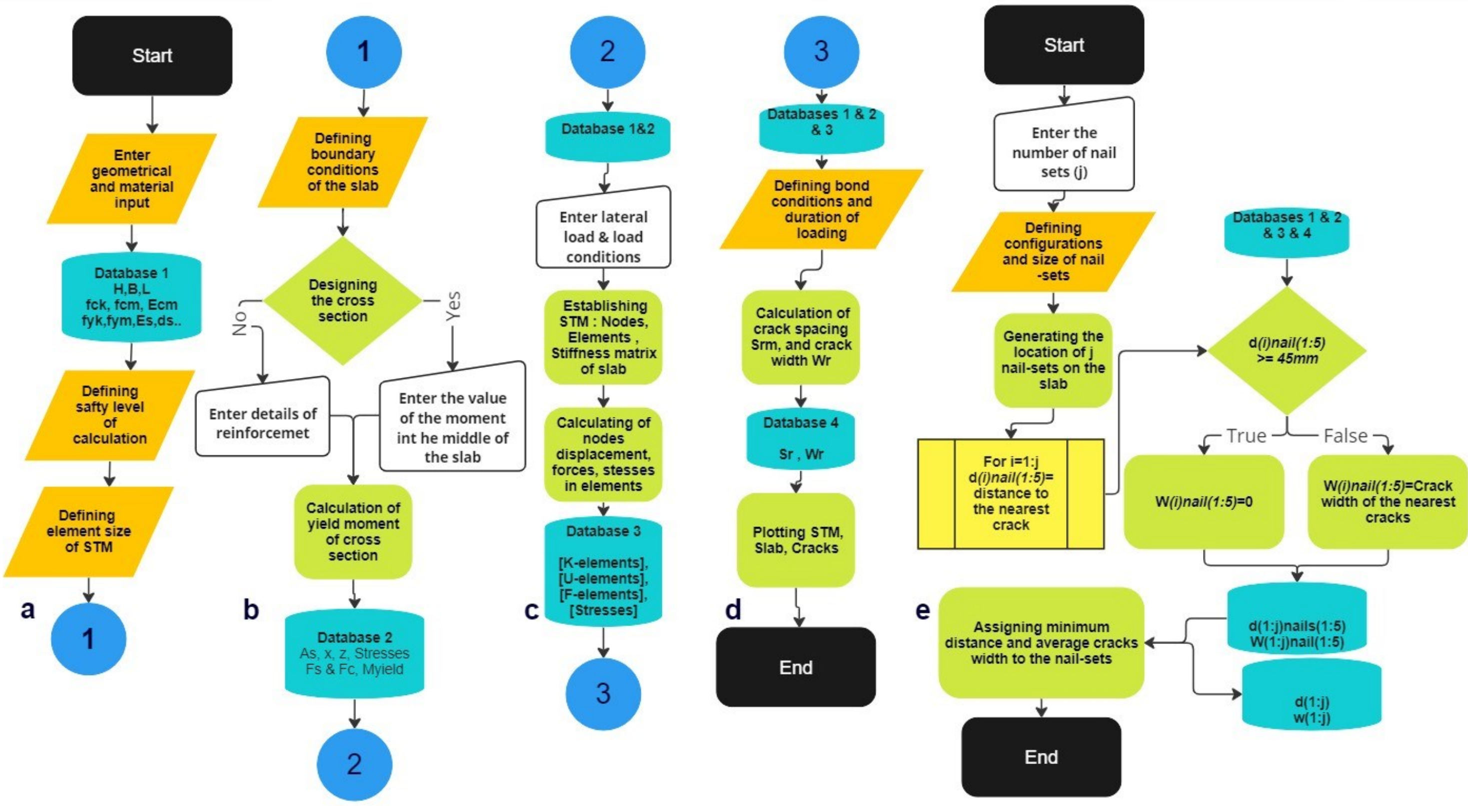

Figure 4. a: "Input". b:" Yielding moment". c: "Strut and tie model". d: "Calculation of crack width". e:" Generating nails-sets".

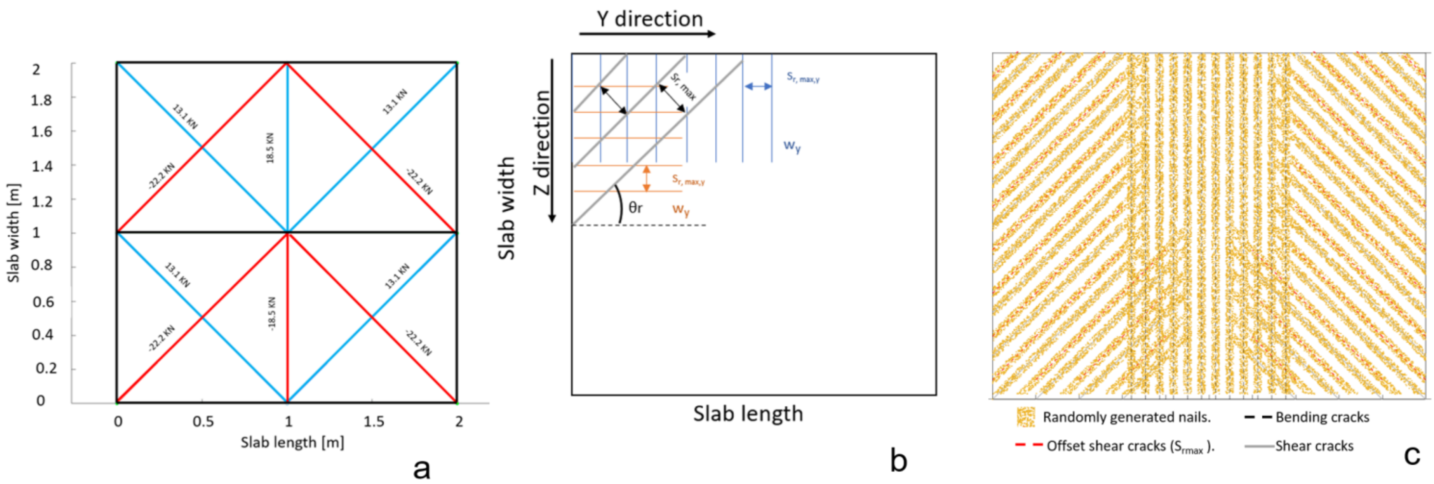

Figure 5. a: Tension and compression paths in the plane of the slab due to the strut and tie model. b: calculation of diagonal cracks. c: Nails located within the influence zone of the cracks (specifically, within 45 mm from each side of the cracks).

4.2. Comparative assessment for the flexural and shear cracks with results from NLFEM software ATENA

ATENA, a concrete simulation software, validated the calculation tool using a 5.25 m x 4 m reinforced concrete slab. The concrete has a compressive strength (f_{ck}) of 45 MPa, tensile strength (f_{ct}) of 3.6 MPa, and an elasticity modulus (E_c) of 31476 MPa. The steel rebars are 3 Φ 10 mm bars per 1 meter, with a steel elasticity modulus (E_s) of 199900 MPa. The limit state is defined by flexural cracks at the steel yielding moment in the center of the slab and shear cracks at the steel yielding force due to planar shear. The cracks are modeled according to the EC2 standard. Both software and the TU model were compared for flexural and shear crack patterns and values. The results indicate a good correspondence in terms of crack patterns and crack widths for both cases. Figure 7 illustrates the results in both ATENA software and the MATLAB model.

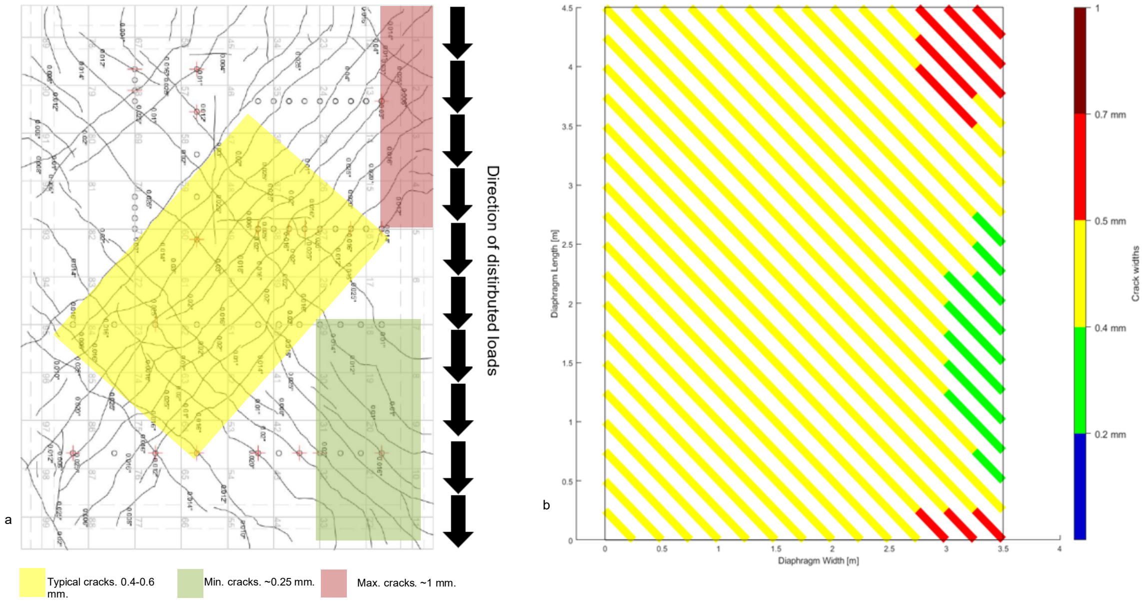

Figure 6. a: Test results Avellaneda, R (2021). b: Simulation of experimental test Avellaneda, R (2021) in MATLAB model.

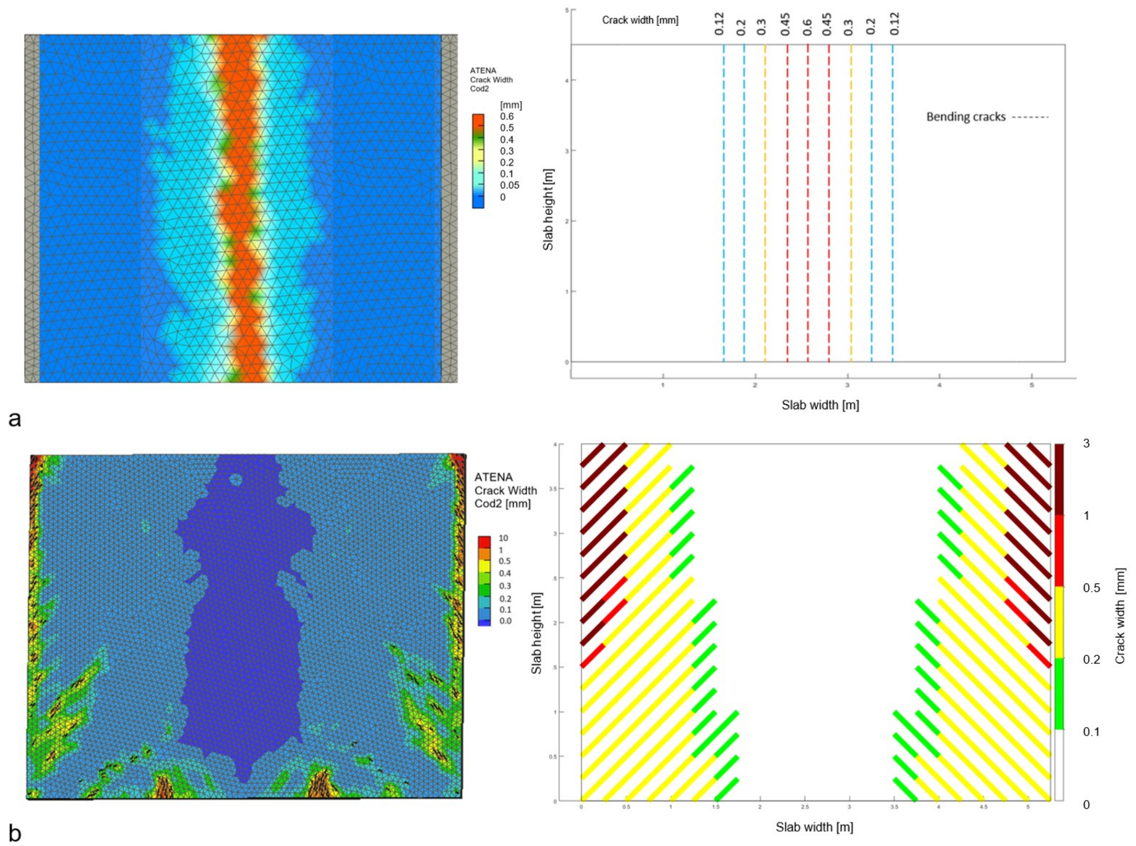

Figure 7. Comparative assessment for flexural and shear cracks in ATENA(Left) and MATLAB model (Right). a: Flexural cracks. b: Shear cracks.

5. Parametric and probabilistic evaluation of set of common concrete slab configurations

In this section, a statistical assessment of shear and flexural cracks was conducted for a set of 12 concrete slabs. Table 1 displays the 95% fractile of crack widths, within which or in their influence zone nails were generated. All selected slabs are sharing a common material configuration commonly used in practice (as outlined in Table 1). These slabs maintain the same material configuration, C30/37 concrete, and steel class B500C minimum. Crack calculations were performed using the EC2 crack model, assuming a "good" bond condition, and conducted under short-term loading conditions. Each slab features symmetric upper and lower reinforcement. The distinguishing factor among them lies in their geometric configurations, which are detailed in Table 1. An additional sensitivity analysis was carried out, emphasizing the impact of the size and orientation of nail sets (Figure 8a), the number of generated nail sets required to stabilize the 95% value (Figure 8b), In the sensitivity analysis, it has been also revealed that the assumption regarding crack spacing S_{rmax} leads to the highest value of the 95% quantile.

From Figure 8, it is evident that the vertical (Parallel to the short side of the slab) and smaller nail sets tend to give a larger 95% quantile of crack widths. Similarly, employing the maximum crack spacing tends to result in higher values for the 95% fractile of cracks. The sensitivity analysis reveals that when the number of nail sets exceeds 1000, it stabilizes the calculation of the 95% value of the nail sets. These assumptions will be taken into account for the calculation of all the other slabs.

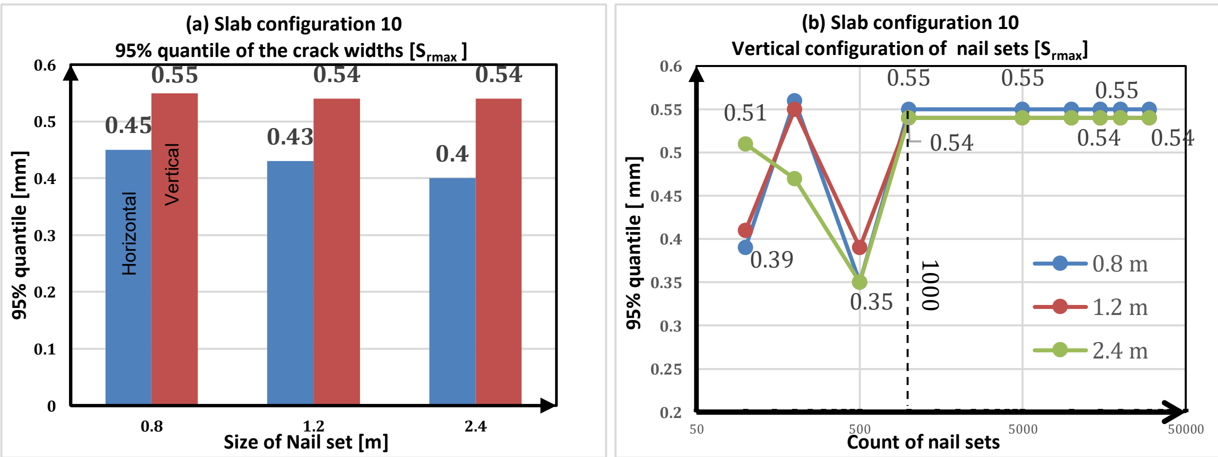

Figure 8. Sensitive analysis. a: Nail set size and orientation. b: Count of nail sets.

Table 1 shows that, the crack widths in cases 6, 9, 10, 11, and 12 are noticeably greater compared to the other cases. This is mainly due to the greater load required to reach failure in these cases, which is a consequence of the thicker slab configuration. Cases 5, 7, and 8, on the other hand, have smaller crack widths, and this can be attributed to a higher reinforcing ratio and a smaller concrete cover, even though the slab thickness remains the same. The results highlight that assuming "steel yielding in the model (Seismic cracking limit state)," a similar approach as used by Hoehler (2006), results in the largest 95% quantile and mean crack widths. It's important to note that crack widths in slabs are typically smaller than those in beams and columns.

Table 1. Summary of the configuration and results.

Slab configuration*						Nailset (5000 Horizontal & 5000 vertical)					
						Crack width (EC2) due to Load assumption [mm]					
Slab con.	**Slab thickness**	**Bar diameter**	**Bar spacing**	**Reinf. Ratio**	**Crack spacing**	**Diaphragm shear strength**			**Steel yielding in shear**		
	[mm]	[mm]	[mm]	[-]	[mm]	$Q_{95\%}$	M_v^*	Std*	$Q_{95\%}$	M_v^*	Std*
1	100	14	65	0.049	102	**0.20**	0.10	0.062	**0.34**	0.20	0.103
2	100	14	130	0.025	117	**0.25**	0.10	0.075	**0.29**	0.14	0.092
3	100	20	65	0.101	95	**0.20**	0.10	0.054	**0.40**	0.20	0.118
4	100	20	130	0.050	124	**0.23**	0.10	0.067	**0.50**	0.20	0.130
5	250	14	65	0.020	145	**0.28**	0.10	0.082	**0.40**	0.20	0.111
6	250	14	130	0.010	325	**0.35**	0.10	0.111	**0.40**	0.20	0.140
7	250	20	65	0.040	128	**0.24**	0.10	0.070	**0.45**	0.20	0.140
8	250	20	130	0.020	178	**0.33**	0.15	0.080	**0.50**	0.25	0.150
9	250	14	65	0.020	225	**0.43**	0.15	0.120	**0.53**	0.25	0.170
10	250	14	130	0.010	325	**0.50**	0.20	0.160	**0.51**	0.20	0.160
11	250	20	65	0.040	200	**0.38**	0.13	0.110	**0.60**	0.30	0.200
12	250	20	130	0.020	270	**0.48**	0.15	0.130	**0.58**	0.15	0.190

***2-way reinforcing. Steel B500C. C30/37. Influence zone on fasteners around the crack: 45 mm (in a distance of 45 mm or less the fastener is considered to be in the cracks). Concrete cover Case (1 to 8) : 20 mm. Concrete cover Case (9 to12): 45 mm. Q95%: 95% quantile of the crack widths. Mv: the arithmetic mean value of the crack widths. Std: Standard deviation.[1]Maximum Crack spacing is considered for each configuration individually.**

6. Conclusion

Direct fastening by the use of nail-type Power Actuated Fasteners (PAFs) is commonly used for light-duty steel and concrete applications like interior partitions. However, its behavior under seismic conditions lacks sufficient data. There is also a lack of seismic criteria for such fastening systems. Since the load-bearing capacity of PAFs is significantly affected by the development of cracks in concrete, it is required to investigate statistically the cracking development under seismic assumptions and its intersection with PAFs' installation positions on concrete floor slabs. The focus here is on its application for non-structural interior partition walls. This Paper aims to simulate seismic crack patterns in concrete floor slabs using a MATLAB model. This model considers various configurations and incorporates a comprehensive database of standard materials. A statistical investigation of crack widths in typical fastening patterns for interior partition walls is also conducted by generating a random nail set. To validate our results, a comparison is made with existing studies and experiments. Critical nail configurations are defined through a parametric sensitivity analysis. The evaluation covers 12 cases with common configurations and the parametrised output is summarised in Table 1. The main conclusions drawn from this study are summarised as follows:

1. Efficiency of Strut and Tie Method (STM): The STM is identified as an efficient approach for accurately capturing the cracking behaviour in concrete, supported by tests, numerical simulations, and analytical modelling.
2. Suitability of EC2 Crack Model: The crack model provided by EC2 is deemed suitable for realistically representing cracking behaviour in concrete floor diaphragms, both due to planar shear and in localized areas near the yield stress of steel.

3. Influence of PAF Set Size and Orientation: The size and orientation of installed PAF sets significantly influence the upper range of crack widths associated with the 95% fractile of the PAFs. Vertical PAF sets and smaller configurations tend to produce larger crack widths within their influence zones.
4. Influence Zone for Cracks: Tests indicate that a 45 mm zone around cracks is adequate for considering nails in cracked concrete. Sensitivity analysis shows minimal impact on results with theoretical increases in the influence zone beyond 45 mm.
5. Probabilistic Investigations: The upper range of crack widths within which 95% of installed nails are located is limited to 0.25 mm for slabs up to 100 mm thickness in diaphragm shear limit state and 0.5 mm at the steel yielding in shear limit state. For slabs up to 250 mm thickness, the upper range is limited to 0.5 mm in diaphragm shear and 0.6 mm in steel yielding in planar shear.

7. References

ASCE (2016). Minimum Design Loads for Buildings and Other Structures ASCE/SEI 7-16, American Society of Civil Engineers (ASCE).

Avellaneda, R; Eatherton, M; (2021). Cantilever diaphragm test of a solid reinforced concrete slab with hilti power actuated fasteners; VirginiaTech; Report No. CE/VPI-ST-21/03.

Červenka, J., Červenka, V., & Laserna, S. (2018). On crack band model in finite element analysis of concrete fracture in engineering practice. Engineering Fracture Mechanics, 197, 27-47.

DIN EN 1992-1-1 (2011) Eurocode 2: Bemessung und Konstruktion von Stahlbeton- und Spannbetontragwerken - Teil 1-1: Allgemeine Bemessungsregeln und Regeln für den Hochbau. Berlin: Beuth Verlag.

Eatherton, M; Avellaneda, R; Grzesik, P; Gill; C;(2006). Crack widths in concrete floor diaphragms, in relation to selected Power Actuated Fasteners used to attach interior partition walls; Fifth International Workshop, SPONSE.

Faraone, Gloria; Hutchinson, Tara C; Piccinin, Roberto; Silva, John. ACI Structural Journal; Farmington Hills Vol. 116, Iss. 6, (Nov 2019): 281-292.

Fib bulletin (2021): Design and assessment with strut-and-tie models and stress fields.

Gribniak, V., Cervenka, V., & Kaklauskas, G. (2013). Deflection prediction of reinforced concrete beams by design codes and computer simulation. Engineering Structures, 56, 2175-2186.

HILTI; 01/2021 .Direct Fastening Technology Manual.

Hoehler, M. (2006) Behavior and Testing of Fastenings to Concrete for Use In Seismic Applications, Dissertation, University of Stuttgart.

Kaufmann, W. (1998) Strength and Deformations of Structural Concrete Subjected to In-Plane Shear and Normal Forces, Dissertation, Institute of Structural Engineering, Swiss Federal Institute of Technology Zurich.

König, G.; Tue, N. V. (1996) Grundlagen und Bemessungshilfen für die Rißbreitenbeschränkung im Stahlbeton und Spannbeton. Heft 466, Deutschen Ausschusses für Stahlbeton.

Marti et al. (1998): Tension chord model for structural concrete, IABSE.

Moehle, Jack P., Hooper, John D., Kelly, Dominic J., and Meyer, Thomas R. (2010). “Seismic design of cast-in-place concrete diaphragms, chords, and collectors: a guide for practicing engineers,” NEHRP Seismic Design Technical Brief No. 3

Rodriguez, M. E., J. L. Restrepo, and J. J. Blandon; (2007). Seismic design forces for rigid floor diaphragms in precast concrete building structures. J. Struct. Eng. 133 (11): 1604–1615.

Taghavi, S; Miranda, E; (2003). Response assessment of nonstructural building elements; Pacific Earthquake engineering research center.

Tue, N. V.; Fehling, E.; Schlicke, D.; Krenn, C. (2021) Rissbreitennachweis und Mindestbewehrung nach EC 2- aktuelles Modell versus Vorschlag für die Revision. . (Crack width verification and minimum reinforcement according to Eurocode 2 – current model versus new proposal for revision) Beton- und Stahlbeton 116, Heft 11, Berlin: Ernst & Sohn Verlag.